



An experimental investigation of the thermal performance of an asymmetrical flat plate heat pipe

Y. Wang, K. Vafai*

Department of Mechanical Engineering, The Ohio State University, 206 West 18th Avenue, Columbus, OH 43210-1107, USA

Received 23 September 1999; received in revised form 20 January 2000

Abstract

An experimental investigation of the thermal performance of a flat plate heat pipe is presented in this work. The results indicate that the temperature along the heat pipe wall surfaces is quite uniform. The results also indicate that the porous wick of the evaporator section creates the main thermal resistance resulting in the largest temperature drop, which consequently affects the performance of the heat pipe. The idea of the heat pipe time constant is introduced in this work to describe the transient characteristics of the flat plate heat pipe and an empirical correlation for the time constant in terms of input heat flux is presented. Correlations for the maximum temperature rise and maximum temperature difference within the heat pipe are also presented. The experimental results at steady state were compared with the analytical results and found to be in good agreement. This work constitutes the first detailed experimental investigation of a flat plate heat pipe. © 2000 Elsevier Science Ltd. All rights reserved.

Keywords: Flat-shaped heat pipes; Thermal performance; Experimental investigation

[1. Introduction

As a high thermal conductor, heat pipes have been used in different applications such as energy conversion, energy storage systems, and electronic cooling. The flat plate heat pipe functions in a substantially different manner as compared to the conventional tubular heat pipes, as it involves a more complex transport mechanism. Due to its favorable thermal characteristics, a flat plate heat pipe finds many applications such as cooling of high power semiconductor chips and cooling of electronic equipment. It also finds applications in spacecraft radiator segments [1,2]

and in the thermal management in the irradiation facility for Boron Neutron Capture Therapy (BNCT) [3–7].

Although the research work on traditional cylindrical and annular heat pipes has been well documented, there is far less work conducted for flat plate heat pipes. Therefore, there is a need to carry out analytical, numerical, and experimental studies for flat plate heat pipes to map out their operational characteristics. In earlier studies by Vafai and his coworkers, both analytical and numerical investigations were conducted for the vapor and fluid flows as well as for the heat transfer characteristics for the startup process of a flat plate heat pipe. Using a detailed and comprehensive analytical method, Vafai and Wang [3] investigated the overall performance of an asymmetrical rectangular flat plate heat pipe. They developed a pseudo-three-dimensional analysis model for steady incompressible

* Corresponding author. Tel.: +1-614-292-6560; fax: +1-614-292-3163.

E-mail address: vafai.1@osu.edu (K. Vafai).

Nomenclature

A	heat input area, m^2
h	thickness
h_{conv}	heat transfer coefficient, $W/m^2 \text{ } ^\circ\text{C}$
k	thermal conductivity, $W/m \text{ } ^\circ\text{C}$
q	heat flux, W/m^2
Q	power input rate, W
t	time, s
t_c	time constant, s
T	temperature, $^\circ\text{C}$
y	normal coordinate
z	normal coordinate
ΔT	temperature difference, $^\circ\text{C}$
ε	porosity
θ	temperature rise, $^\circ\text{C}$

Subscripts

c	condenser
e	evaporator
eff	effective
l	liquid
max	maximum
oc	outside surface of condenser section
oe	outside surface of evaporator section
s	solid
v	vapor
w	wick
wa	wall
wv	wick–vapor interface
ww	wall–wick interface
∞	environment

vapor and liquid flows inside the flat plate heat pipe. Details of the physics of the transport processes within the heat pipe were analyzed and established. They also investigated the maximum heat transfer capacity of the flat plate heat pipe based on capillary limitation.

Employing conservative formulations, Vafai et al. [4] investigated the steady incompressible vapor and liquid flows for a disk shaped heat pipe analytically. They compared the asymmetrical vapor velocity profile, the vapor and liquid pressure distributions, and the vapor temperature distribution in a disk shaped heat pipe with that in a rectangular flat plate heat pipe. Taking into consideration the effect of liquid–vapor coupling and non-Darcian transport, Zhu and Vafai [5] performed a comprehensive investigation for the vapor flow and pressure distribution in the vapor region of a disk shaped heat pipe. The liquid velocity profiles in the porous wicks were obtained using the method of matched asymptotic expansions. The coupling of the liquid flow in the top and the bottom and the coupling of the vapor and the liquid phases were established. They found that there is a vapor reversal flow in the vapor region. In addition, Zhu and Vafai [6] developed an analytical model to predict the transient thermal behavior of the asymmetrical flat plate heat pipes during the startup process. The temperature distributions within the heat pipe walls and liquid-saturated wicks were obtained analytically. Wang and Vafai [7] performed an analysis for startup and shutdown operations of flat plate heat pipes. The dependence of the thermal performance of the flat plate heat pipe on power input and cooling heat transfer coefficient was investigated and the simulation results were presented.

There is a very limited number of experimental investigations available regarding the flat plate heat pipes. Furthermore, these few investigations are found on system specific applications and testing of the flat plate heat pipes. In addition, the heat pipes utilized in these experiments were based on a substantially simpler structure compared to those proposed and analyzed by Vafai et al.

Among the very few experimental investigations in this area, the works of Kikuchi et al. [8], Basiulis et al. [9], and Thomson et al. [1] can be cited. Kikuchi et al. [8] had carried out experiments on an electrohydrodynamic flat plate heat pipe. The heat pipe was 100 cm in length and 10 cm in width, and employed three electrodes. The orientation was horizontal in this study. Freon 11 and 113 were separately used as working fluids. It was found that Freon 11 was superior to Freon 113 from the point of view of thermal transport. Heat transport capabilities up to 150 W were recorded. Basiulis et al. [9] conducted experiments to test the performance of flat plate heat pipes for cooling printed wiring boards. A maximum power input up to 100 W and heat fluxes up to 2 W/cm^2 were reported for the tested heat pipes. Thomson et al. [1] performed experiments to investigate the application of flat plate heat pipes in the cooling of high power amplifiers for communication satellites. The surface temperatures of the heat pipe were measured. No vertical wicks were reported and the condensate return path was not specified. Once again, it should be noted that the heat pipes utilized in these works are simpler in form than that analyzed by Vafai et al. [3,5–7].

In this work, an experimental investigation is conducted to characterize the thermal performance of a

flat plate heat pipe. In order to describe the transient performance of a heat pipe, the concept of heat pipe time constant is introduced. The temperature distribution and heat transfer coefficients are obtained. An empirical correlation for the maximum temperature difference within the heat pipe as well as for the maximum temperature rise both in terms of input heat are presented. Finally, steady state experimental results are compared with the analytical results.

2. Experimental apparatus

Fig. 1 is the schematic of the flat plate heat pipe. The heat pipe is 190.50 mm in length, 139.70 mm in width, and 34.93 mm in thickness. The heat pipe walls were made of 3.175 mm thick copper plate. Attached to the inner surfaces of the heat pipe wall

are porous wicks, as shown in Fig. 1. The vertical wicks provide a secondary return mechanism for the condensate. The vapor region is composed of four identical channels. The wicks were sintered copper powder providing a thickness of 1.651 mm. The pore radius of the wicks was 3.1×10^{-5} m and its porosity was 50%. The permeability of the wick was 7×10^{-12} m².

The evaporation section was located on the center of one of the outside surfaces of the heat pipe. Therefore, the heat pipe can be divided into four sections, i.e., one evaporator section and three condenser sections (Fig. 1). Fig. 2 is the schematic of the experimental setup. During the experiment, the heat pipe was positioned vertically, and thus the same average heat transfer coefficient on the three condensation surfaces is achieved. A Lexan frame of 12.7 mm thick was employed to hold the heat pipe. The function of the

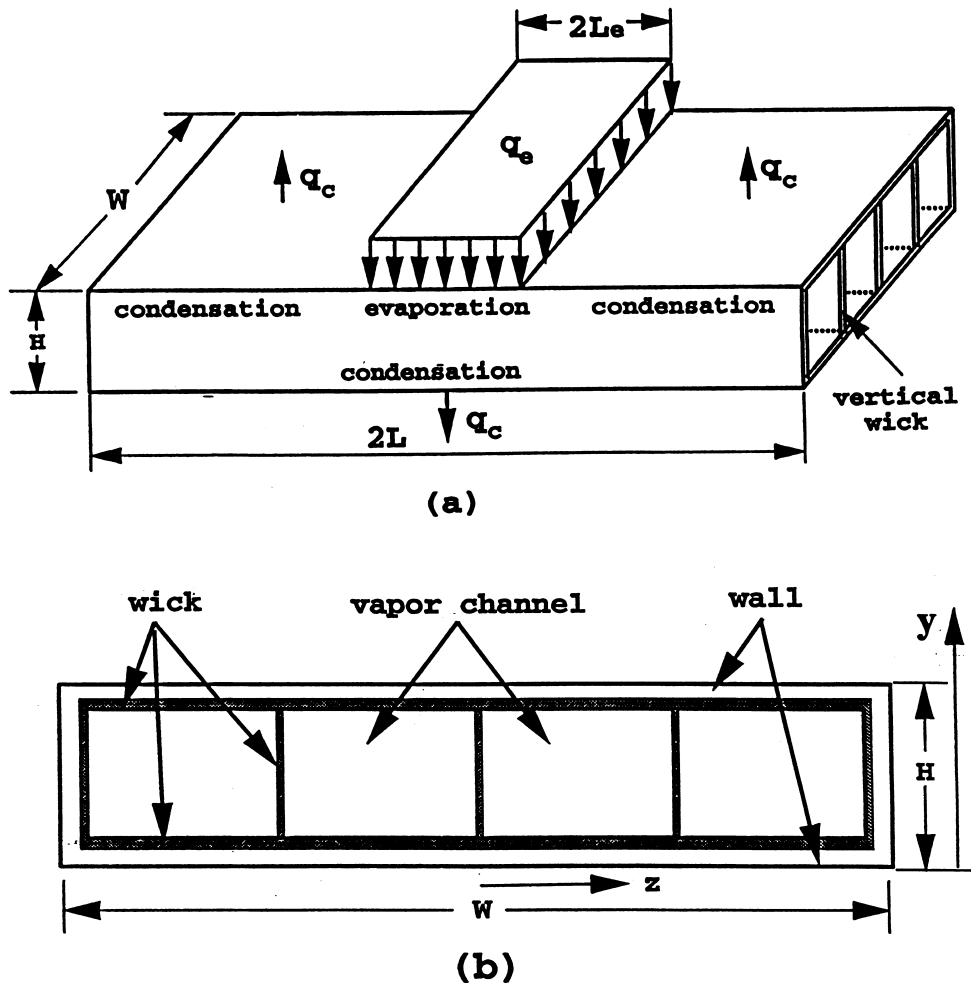


Fig. 1. Schematic of the flat plate heat pipe: (a) geometry of the heat pipe and (b) cross-sectional view of the heat pipe.

Lexan frame was twofold: to support the heat pipe and to reduce the heat loss through the four edges of the heat pipe. Taking thermal expansion into account, the inner dimensions of the frame are made larger than that of the heat pipe's, and a 2 mm thick flexible insulation material was placed between the Lexan frame and the heat pipe. The flexible insulation material allows the heat pipe to expand after its temperature rises. The flexible insulation material can also reduce the heat loss through surfaces other than the previously mentioned three condenser sections of the heat pipe. A support was also employed to raise the Lexan frame to a certain height so as not to affect the free air flow over the outside condenser surface.

A flexible heater (139.7 mm in length and 50.8 mm in width), specially designed for this experiment (Watlow Company), was attached on the center of the top heat pipe surface. The other side of the heater was insulated (Fig. 2). Thirty E-type thermocouples were installed to measure the outside surface temperatures of the heat pipe with 15 on each surface of the heat

pipe. A 6 mm × 0.3 mm groove was machined in the heat pipe walls and a high conductivity cement was utilized to embed the thermocouples within the heat pipe wall. The spacing between adjacent thermocouples was 12.7 mm, except for the thermocouples at the end, which were separated 19.1 mm from each other, as shown in Fig. 2.

In order to monitor the heat loss through the insulated surfaces, thermocouples were also installed on both the inner and outer surfaces of the Lexan frame. The room temperature was also measured with two E-type thermocouples. Power was fed through a power supply (National Instruments) and the temperature data was collected through a data acquisition system. The temperature signal was monitored every second until a steady state was achieved.

3. Data reduction

Under steady state conditions, the heat transfer coefficient on the surfaces of the condenser section can be determined by

$$h = \frac{q_c}{T_{wa, oc} - T_\infty} \quad (1)$$

where $T_{wa, oc}$ is the average temperature of the outside surface of the wall of the condenser section and q_c is the output heat flux from the condenser section given by,

$$q_c = \frac{Q}{A_c} \quad (2)$$

where A_c is the total area of the condenser section. The input heat flux in the evaporator section is

$$q_e = \frac{Q}{A_e} \quad (3)$$

where Q is input power and A_e is the area of the evaporator section. Based on the measured average temperature of the outside surface of the evaporator wall $T_{wa, oe}$, $T_{wa, oc}$, and the input heat flux q_e , the temperatures at the solid–liquid and liquid–vapor interfaces are obtained:

$$T_{ww, e} = T_{wa, oe} - \frac{q_e h_{wa}}{k_{wa}} \quad (4)$$

$$T_{wv, e} = T_{ww, e} - \frac{q_e h_w}{k_{eff}} \quad (5)$$

$$T_{ww, c} = T_{wa, oc} + \frac{q_c h_{wa}}{k_{wa}} \quad (6)$$

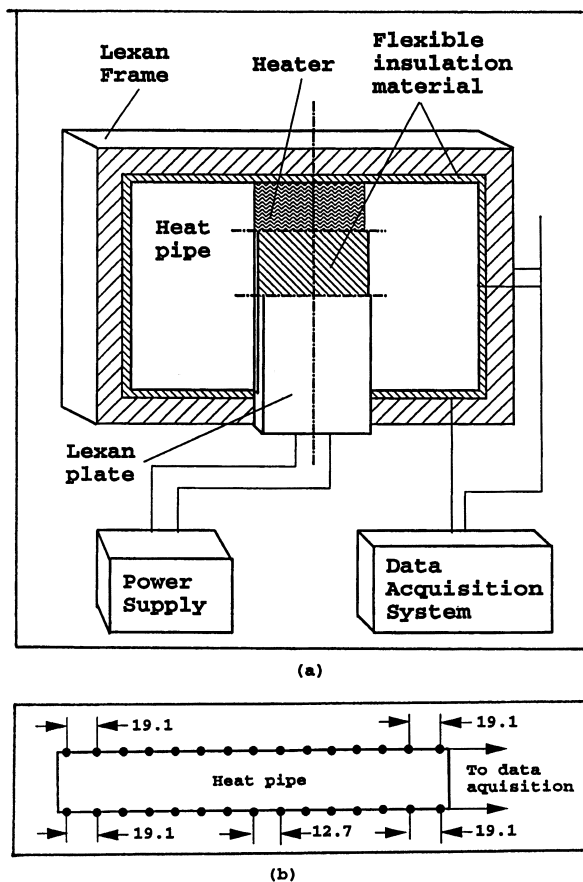


Fig. 2. Experimental system: (a) experimental setup and (b) location of the embedded thermocouples.

$$T_{wv, c} = T_{wv, e} + \frac{q_c h_w}{k_{eff}} \tag{7}$$

According to Tournier et al. [10] and Zhu and Vafai [4], the temperature variation within the vapor phase is very small and thus can be neglected. The vapor temperature is then taken as

$$T_v = \frac{1}{2}(T_{wv, e} + T_{wv, c}) \tag{8}$$

The effective thermal conductivity for the wick can be found as [11]

$$k_{eff} = k_1 \left[\frac{k_1 + k_s - (1 - \varepsilon)(k_1 - k_s)}{k_1 + k_s + (1 - \varepsilon)(k_1 - k_s)} \right] \tag{9}$$

The measured temperature uncertainty is $\pm 0.1^\circ\text{C}$, the uncertainty of the thickness of the heat pipe wall and wick is ± 0.001 mm, and the uncertainty of the heat pipe length, width, and thickness is ± 0.01 mm. Based on an error analysis [12], the uncertainty for the input power is found to be $\pm 1.7\%$ and the uncertainty in measuring the heat transfer coefficient is found to be $\pm 5.6\%$.

4. Results with discussion

The temporal temperature distribution on the outside wall surface of the flat plate heat pipe for various input heat fluxes is shown in Fig. 3. As can be seen in Fig. 3, for higher input power, the startup time is substantially shorter. The total heat transfer coefficient on the condenser section, obtained from Eq. (1), is plotted as a function of the input heat flux in Fig. 4. As can be seen in Fig. 4, the heat transfer coefficient is relatively constant in the condenser section. The average total heat transfer coefficient under steady state conditions was found to be $12.4 \text{ W/m}^2 \text{ }^\circ\text{C}$ for surface temperatures between 30 and 49°C , with a maximum predicted relative error of $\pm 7\%$.

The measured maximum surface temperature is plotted against the input heat flux in Fig. 5. Based on a heat conduction model, which takes into account the room temperature, input heat flux, heat transfer coefficient and the thermophysical and geometric parameters of the heat pipe, the temperature distribution under steady-state conditions in the flat plate heat pipe can be determined analytically. The analytical results are also plotted in Fig. 5. As can be seen in Fig. 5, the

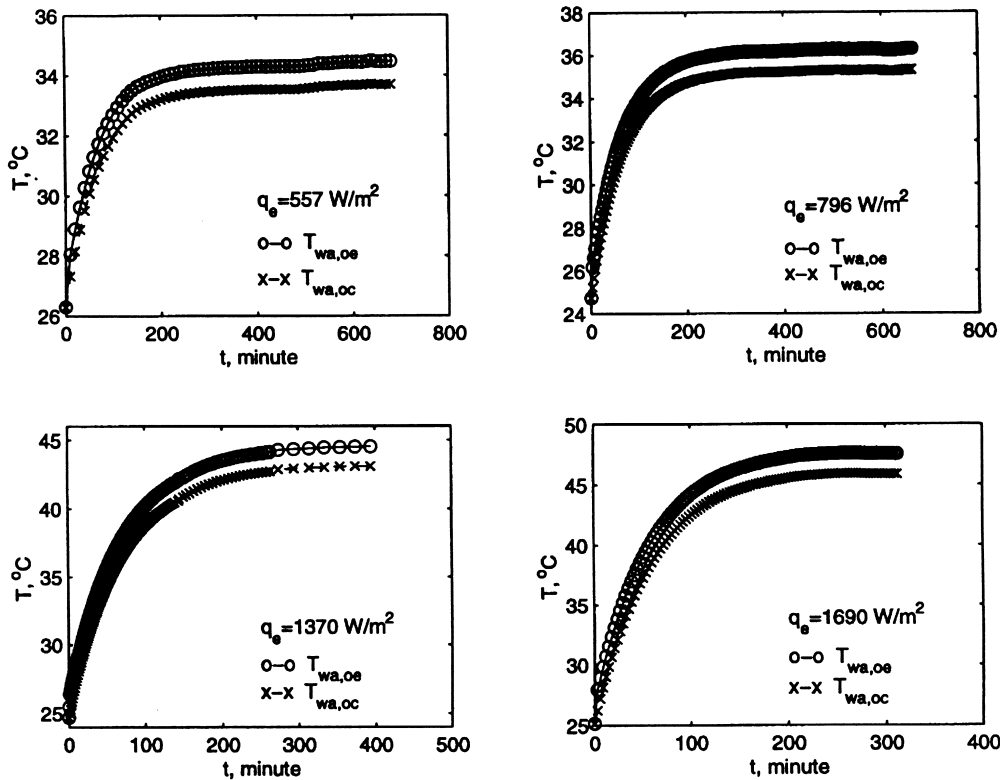


Fig. 3. Transient temperature response of the heat pipe.

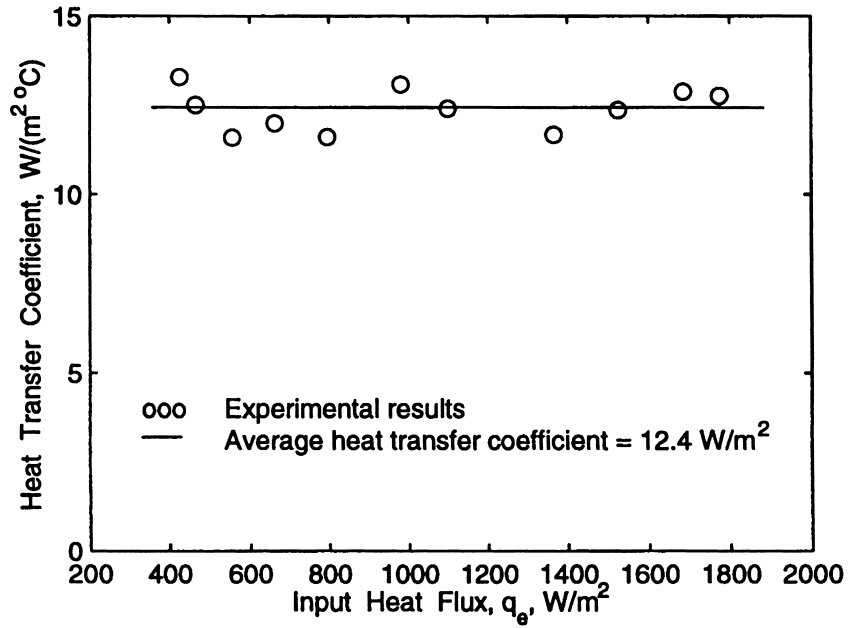


Fig. 4. Heat transfer coefficient dependency on the input heat flux.

maximum temperature increases with an increase in the input heat flux and the measured temperatures were found to be in good agreement with the analytical results. The measured and the analytical surface temperature rise on both the evaporator and condenser

sections are plotted in Fig. 6. As can be seen, the measured temperature rise is in good agreement with the analytical results. Based on the experimental data, an empirical correlation for the maximum temperature rise in terms of the input heat flux is obtained as

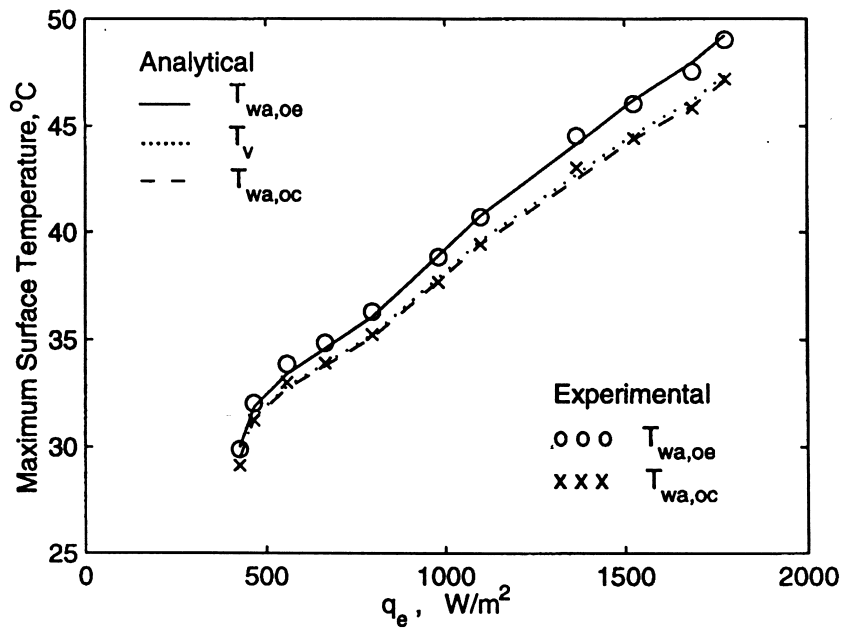


Fig. 5. Effect of the input heat flux on the maximum surface temperature.

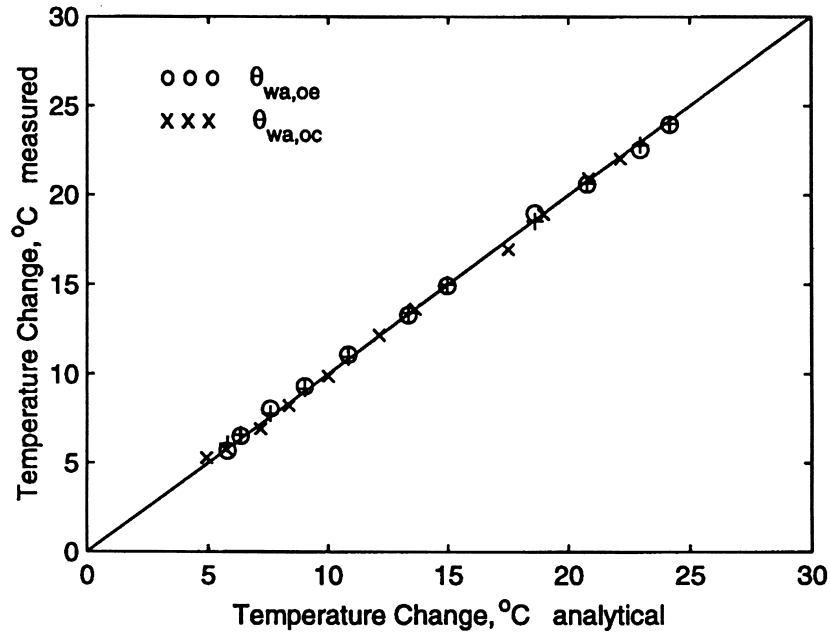


Fig. 6. Comparison of the measured and predicted maximum surface temperature change.

$$\theta_{\max} = 0.376 + 0.0133q_e \quad (10)$$

The maximum temperature difference within the heat pipe is shown in Fig. 7, which shows that the maximum temperature difference increases linearly with the

input heat flux. As can be seen in Fig. 7, the maximum difference between the analytical and the experimental results is about $\pm 0.2^\circ\text{C}$ while the uncertainty in the measured temperatures was $\pm 0.1^\circ\text{C}$. A correlation for the maximum temperature difference within the heat

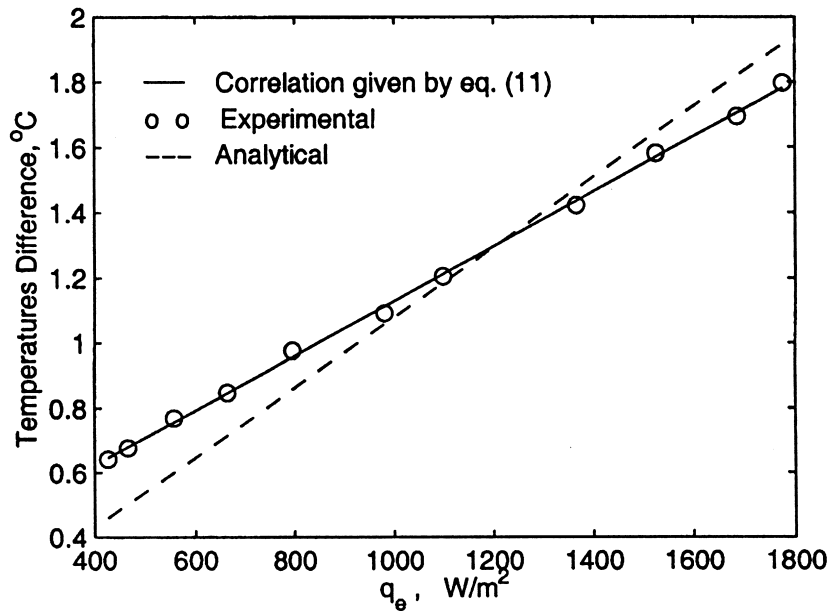


Fig. 7. Effect of input heat flux on the maximum temperature difference.

pipe in terms of the input heat flux can be presented as

$$\Delta T_{\max} = 0.289 + 8.40 \times 10^{-4} q_e \quad (11)$$

The temperature gradients across the heat pipe are shown in Fig. 8. As can be seen in Fig. 8, the temperature gradients across the heat pipe were quite small, which is one of the main characteristics of a flat plate heat pipe. Fig. 8 also shows the contribution of the heat pipe walls and wicks to the total temperature drop for different input heat fluxes. As expected for a copper or aluminum heat pipe, the temperature drop across the heat pipe wall is much smaller than that across the wicks due to the heat pipe wall's substantially larger thermal conductivity (Fig. 8). Therefore, reducing the temperature drop across the wicks, especially in the evaporator section, is essential in improving the performance of the heat pipe.

The temperature distributions along the heat pipe surfaces are plotted at different times in Fig. 9. Once again, it can be seen that the temperature was quite uniform on the largest outside surface of condenser wall. For the outside surface of the evaporator, where the input power is applied, the temperature variation is

small. This is another favorable feature of a flat plate heat pipe as compared to a conventional heat pipe. This feature can be used to remove hot spots produced by arrays of heaters, or to design an efficient radiator. Fig. 10 displays the analytical and experimental temperature distributions of the heat pipe along the z -direction at steady state. As shown in Fig. 10, the analytical results agree with experimental results very well. Detailed aspects related to transient characteristics of flat plate heat pipe during startup and shutdown operations as well as comparisons of experimental and analytical results presents in Ref. [7] are given in Wang and Vafai [13]

The response time to an input power is an important characteristic of a heat pipe. In this regard, the idea of a heat pipe time constant, t_c , was utilized in this work. This constant is defined as the time it takes for the outside surface temperature rise in the evaporator section to reach 63.2% of its maximum value. A small time constant means that the heat pipe can quickly reach its largest work capacity. The measured time constant was plotted against input heat flux in Fig. 11. As shown in Fig. 11, the time constant varies from 58 to 82 min under the present experimental conditions.

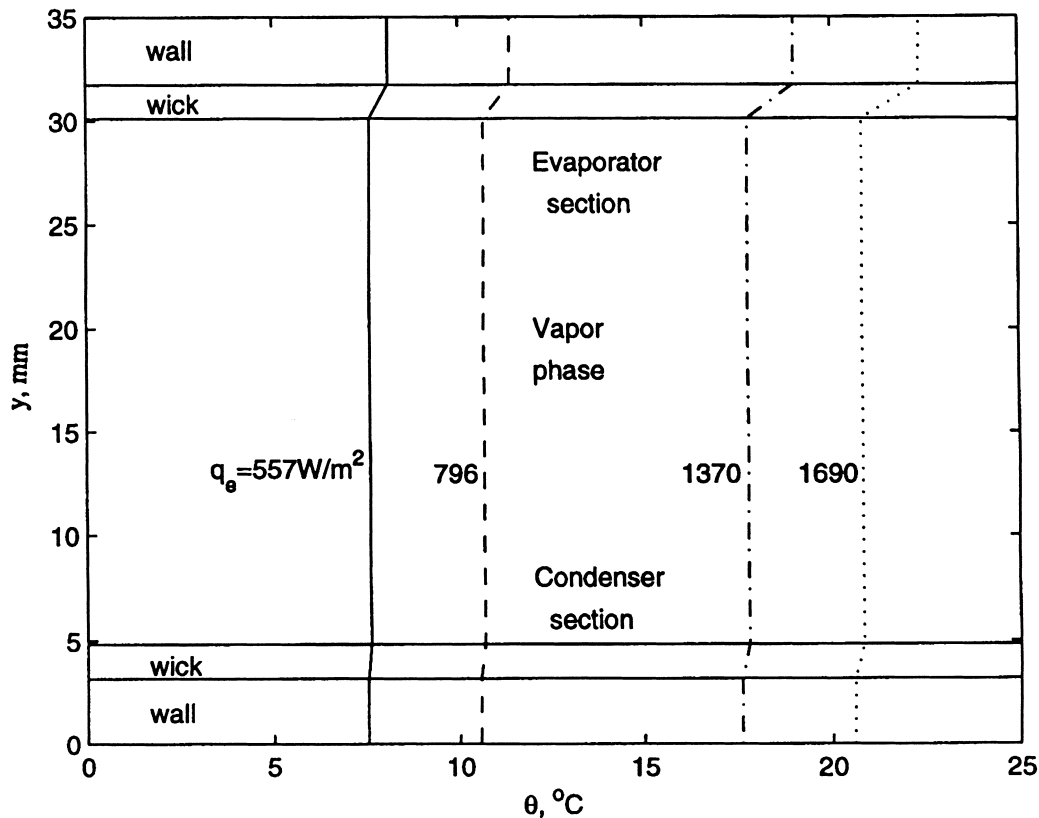


Fig. 8. Temperature drop across the heat pipe.

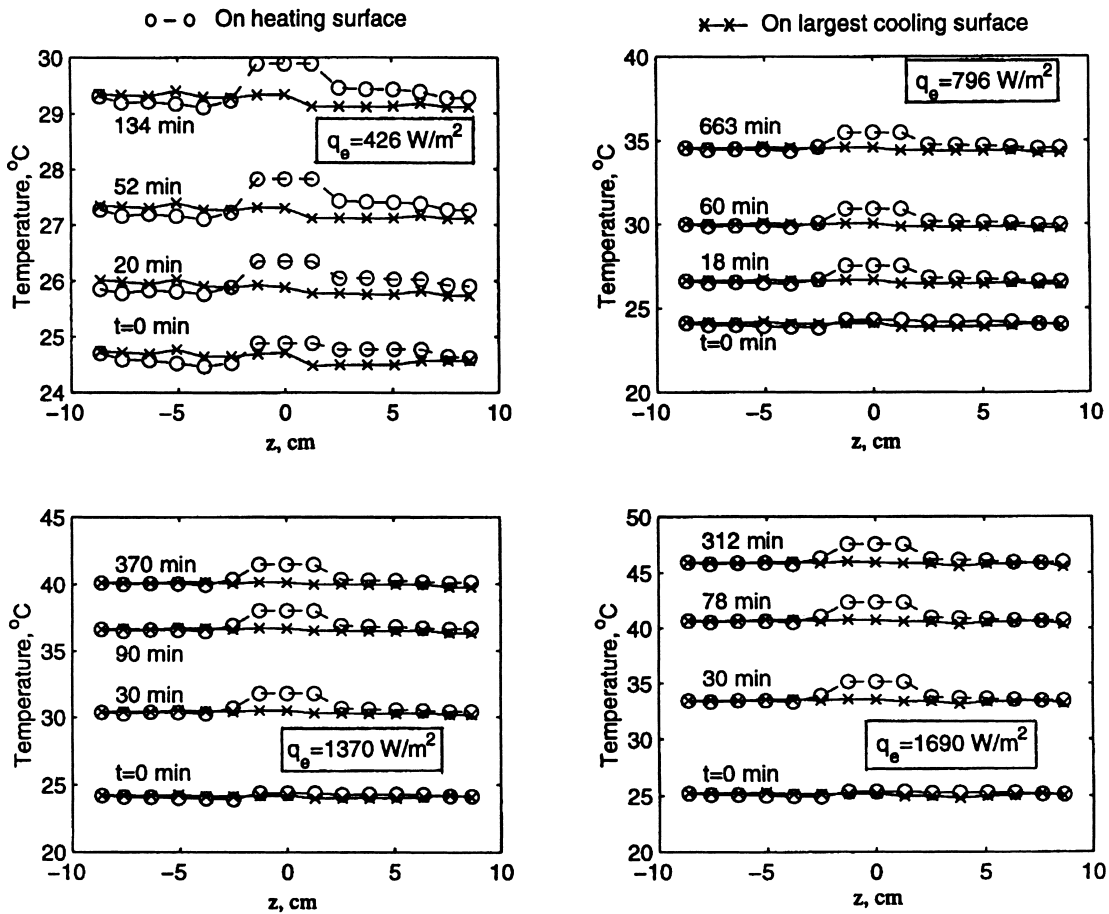


Fig. 9. Temperature distribution along the heat pipe surfaces.

Obviously, input power, the heat transfer coefficient, the temperature difference between the outside wall surface in the condenser section and the cooling fluid, and the heat capacity of the heat pipe affect the time constant. For a specified heat pipe, if the heat transfer coefficient is a constant, heat flux will have a strong effect on the time constant, as can be seen in Fig. 11. For a constant heat transfer coefficient, a larger heat flux will result in a smaller time constant. An empirical correlation for the experimental range is

$$t_c = 91.4 - 0.0339q_e + 8.33 \times 10^{-6}q_e^2 \quad (12)$$

5. Conclusions

An experimental investigation of the thermal performance of a flat plate heat pipe is presented in this work. The results show that the temperature difference within the heat pipe is small and that the

temperature distribution along the heat pipe surfaces in the condenser section is quite uniform. The results also show that the porous wick in the evaporator section constitutes the main thermal resistance resulting in a larger temperature drop as compared to the other layers within the heat pipe. The heat transfer coefficient in the condenser section is calculated based on the experimental data. The average heat transfer coefficient is found to be $12.4 \text{ W/m}^2 \text{ } ^\circ\text{C}$ for input heat flux in the range of $425\text{--}1780 \text{ W/m}^2$.

The idea of a heat pipe time constant is introduced to describe the transient characteristics of a heat pipe. The results show that the time constant varies from 58 to 84 min for the present experimental setup. Based on the experimental results, an empirical correlation for time constant in terms of input heat flux is presented. An empirical correlation for the maximum temperature change and the maximum temperature difference within the heat pipe both in terms of input heat flux are also presented. The steady state experimental

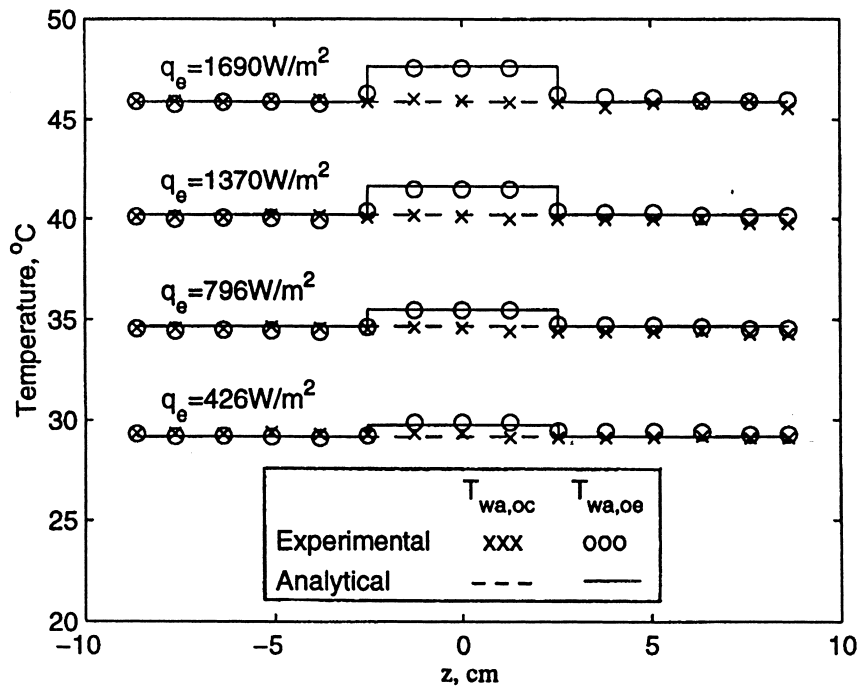


Fig. 10. Surface temperature distribution at steady state.

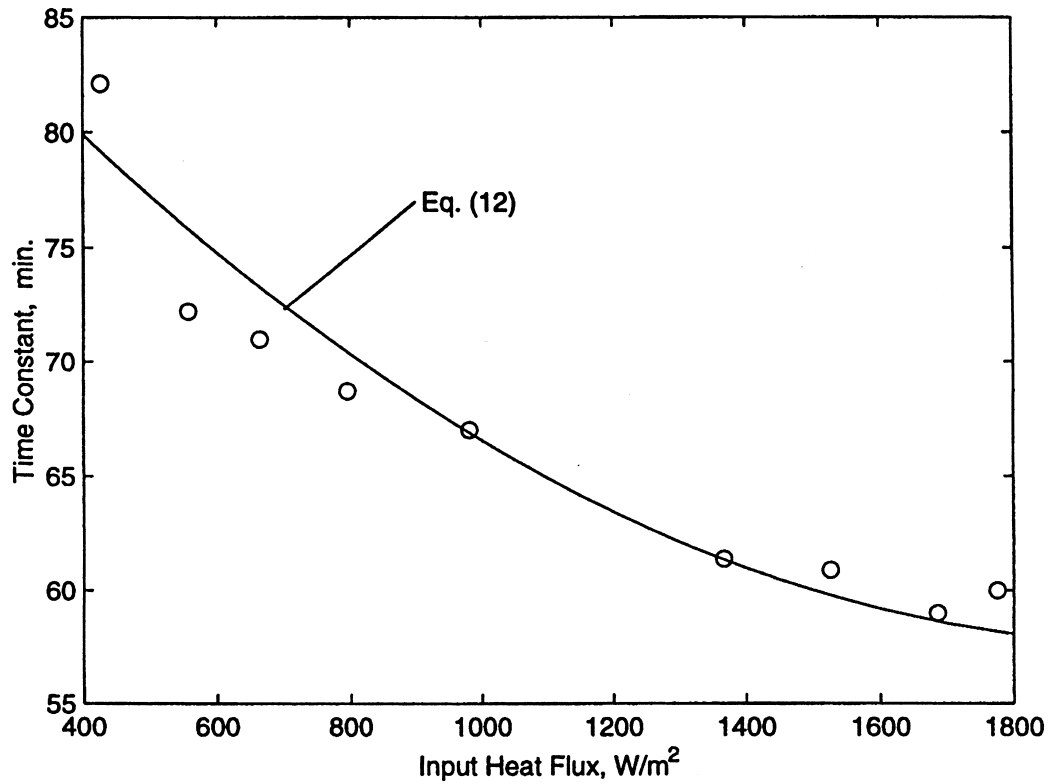


Fig. 11. Effect of input heat flux on the time constant.

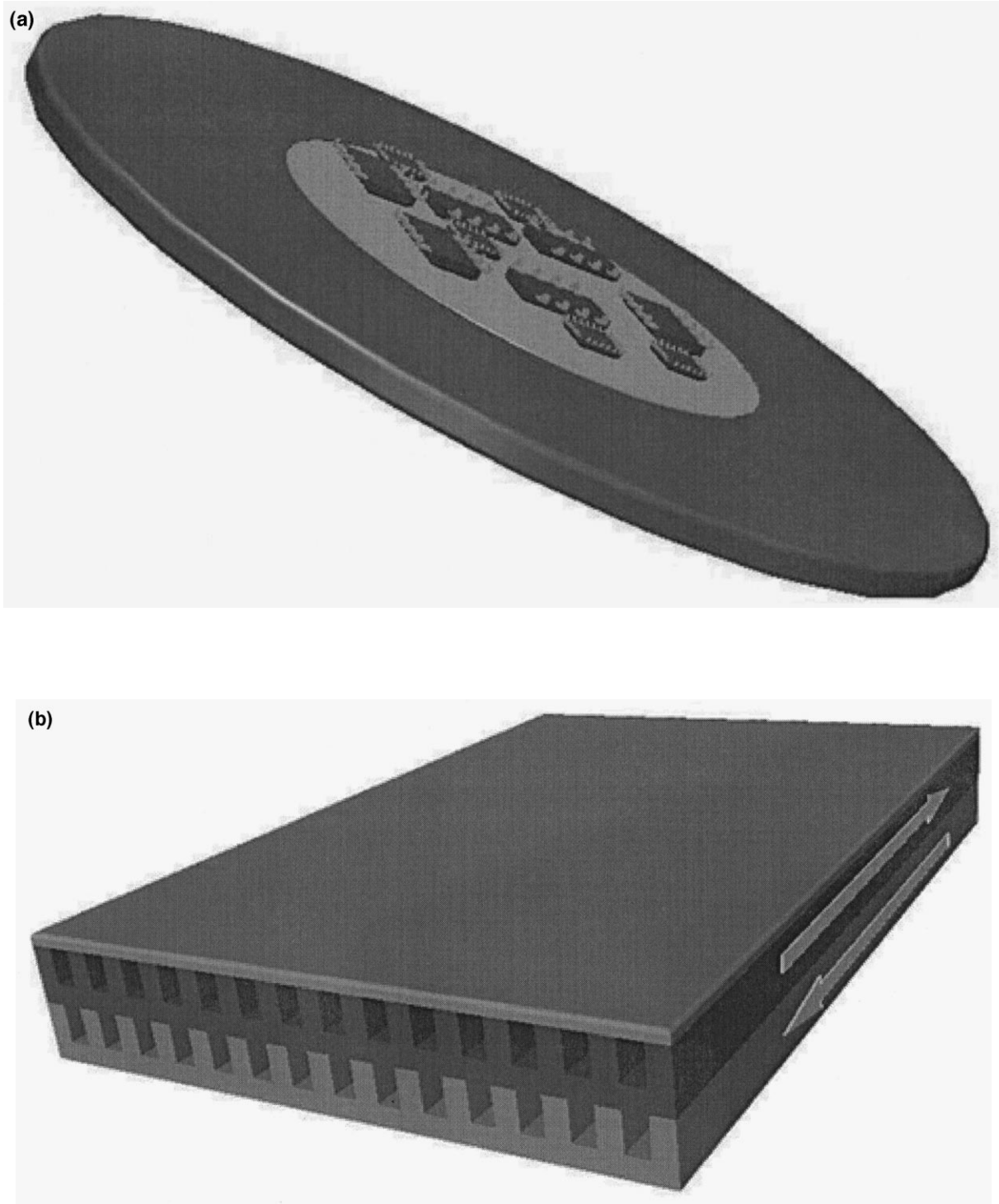


Fig. 12. A conceptual design for electronic cooling using a combination of (a) flat-shaped heat pipe (either disk-shaped or a flat plate) and (b) two-layered micro-channel concept.

results are in good agreement with the analytical results.

A conceptual design for high heat flux cooling using a combination of flat-shaped heat pipe and a two-layered micro-channel concept introduced in Zhu and Vafai [14] can be seen in Fig. 12.

Acknowledgements

The grant (DE-F602-93ER61612) by the Department of Energy is acknowledged and greatly appreciated.

References

- [1] P.D. Dunn, D.A. Reay, *Heat Pipes*, 3rd ed., Pergamon Press, New York, 1982.
- [2] M. Thomson, C. Ruel, M. Donato, Characterization of a flat plate heat pipe for electronic cooling in a space environment, in: 1989 National Heat Transfer Conference, Heat Transfer in Electronics, HTD-Vol. 111, 1989, 59–65.
- [3] K. Vafai, W. Wang, Analysis of flow and heat transfer characteristics of an asymmetrical flat plate heat pipe, *International Journal of Heat Mass Transfer* 35 (1992) 2087–2099.
- [4] K. Vafai, N. Zhu, W. Wang, Analysis of asymmetrical disk-shaped and flat plate heat pipes, *ASME Journal of Heat Transfer* 117 (1995) 209–218.
- [5] N. Zhu, K. Vafai, Vapor and liquid flow in an asymmetrical flat plate heat pipe: a three-dimensional analytical and numerical investigation, *International Journal of Heat Mass Transfer* 41 (1998) 159–174.
- [6] N. Zhu, K. Vafai, Analytical modeling of the startup characteristics of asymmetrical flat plate and disk-shaped heat pipes, *International Journal of Heat and Mass Transfer* 41 (1998) 2619–2637.
- [7] Wang, Y., Vafai, K., Transient characterization of flat plate heat pipes during startup and shutdown operations, *International Journal of Heat and Mass Transfer* 43 (2000) 2641–2655.
- [8] K. Kikuchi, et al., Large scale EHD heat pipe experiments, in: D.A. Reay (Ed.), *Advances in Heat Pipe Technology*, Proc. IV Int. Heat Pipe Conference, Pergamon Press, Oxford, 1981.
- [9] A. Basiulis, H. Tanzer, S. McCabe, Thermal management of high power pwbs through the use of heat pipe substrates, in: Proc. 6th Annual International Electronic Packaging Conference, San Diego, CA, 1986, pp. 501–515.
- [10] J.-M. Tournier, M.S. EL-Fenk, A heat pipe transient analysis model, *Int. J. Heat Mass Transfer* 37 (1994) 753–762.
- [11] S.W. Chi, *Heat Pipe Theory and Practice*, Hemisphere, Washington, DC, 1976.
- [12] S.J. Kline, F.A. McClintock, Describing uncertainties in single sample experiment, *Mechanical Engineering* 75 (1953) 3–8.
- [13] Y. Wang, K. Vafai, An investigation of the transient characteristics of a flat plate heat pipe during startup and shutdown operations, accepted for *ASME Journal of Heat Transfer*.
- [14] K. Vafai, L. Zhu, Analysis of a two-layered micro-channel heat sink concept in electronic cooling, *International Journal of Heat and Mass Transfer* 42 (1999) 2287–2297.